

Temperature dependence of distortion in poly(ethylene oxide) crystals

Yasuo Saruyama

Department of Physics, Kyoto University, Kyoto, Japan

(Received 2 December 1981; revised 30 April 1982)

X-ray studies of poly(ethylene oxide) crystals have been made on integrated intensities of 31 Bragg peaks and the diffraction profile of 120 reflection, which gives information about lateral molecular packing, over the temperature range from -150° to 50°C . Both the integrated intensities of 25 Bragg peaks and the integral breadth of 120 reflection have maxima in their temperature changes. These unusual temperature changes can be attributed to static crystal distortion: static displacement of atoms from their average positions over all crystals. Thermal vibration actually takes place around the displaced positions. Many Bragg peaks were required to be investigated in order to study the effect of the static distortion on the integrated intensities, since temperature changes of the displaced positions lead to changes of both the average positions (crystal structure) and magnitude of the static displacement. A model for the static displacement is proposed; intermolecular interaction is the origin of the static displacement, which is decreased with increasing temperature by a smearing-out effect on the intermolecular interaction due to thermal vibration. Fourier analysis of the profile of 120 reflection suggests that crystalline order is maintained at short range, 20 molecules or more in diameter.

Keywords Polymer; poly(ethylene oxide); crystal distortion; temperature change; X-ray diffraction; diffraction profile; Fourier analysis

INTRODUCTION

Displacement of an atom in a distorted crystal from its ideal position ($\mathbf{u}(t)$) is given by the sum of a static displacement (\mathbf{u}_s) and a dynamic one due to thermal vibration ($\mathbf{u}_d(t)$):

$$\mathbf{u}(t) = \mathbf{u}_s + \mathbf{u}_d(t) \quad (1)$$

The average of $\mathbf{u}_d(t)$ over time t is zero, while \mathbf{u}_s vanishes when it is averaged over all atoms in the crystal. The displacement $\mathbf{u}(t)$ depresses integrated intensities of Bragg peaks in X-ray diffraction. In X-ray structure analysis it is assumed that the intensity depression can be expressed by a factor D , when $\mathbf{u}(t)$ is isotropic

$$D = \exp[-2B(\sin \theta/\lambda)^2] \quad (2)$$

where θ and λ are the Bragg angle and the X-ray wavelength, respectively. The coefficient B is dependent on $\mathbf{u}(t)$ and can be divided into two parts, B_s and B_d , corresponding to \mathbf{u}_s and \mathbf{u}_d in equation (1):

$$B = B_s + B_d \quad (3)$$

In this paper, equation (2) for the factor D , which was used in the structure analysis of poly(ethylene oxide) (PEO) crystals¹, is employed together with equation (3).

The coefficient B_d is known to be proportional to the mean square amplitude of thermal vibration \mathbf{u}_d . The coefficient B_s will increase with the mean square of \mathbf{u}_s , but the general formula for the \mathbf{u}_s dependence of B_s has not been available. In an extreme case that \mathbf{u}_s is equal to $\mathbf{u}_d(t)$ at a certain instance (frozen thermal vibration type), the relation between B_d and \mathbf{u}_d holds between B_s and \mathbf{u}_s , too.

Ruland² investigated an important case in which \mathbf{u}_s is expressed as the combination of the distortions of the frozen thermal vibration type and the paracrystal type, and showed the validity of equations (2) and (3).

The width of a Bragg peak, as well as its integrated intensity, can be changed by \mathbf{u}_s ; they can be varied independently of each other by changing the magnitude of \mathbf{u}_s and the correlation between \mathbf{u}_s 's of different atoms. Then both the integrated intensities and the widths of the Bragg peaks must be taken into account for the study of the nature of \mathbf{u}_s .

Reversible temperature change of the widths of the equatorial diffraction peaks were studied in polyethylene (PE) by Katayama³ and in poly(tetrafluoroethylene) (PTFE) by Yamamoto and Hara⁴; some authors proposed modified methods to analyse Katayama's results^{5,6}. The widths of the diffraction peaks decrease with increasing temperature in both materials. The origin of this unusual temperature dependence has not been understood, but it should be noted that temperature change of the integrated intensities, as well as the widths, is important to interpret the results.

It was reported that in PEO crystals intermolecular interaction plays an important role in determination of the average molecular conformation⁷; the term 'average' is added since X-ray structure analysis provides the structure averaged in time and space. PEO is conspicuous by this point in comparison with PE and PTFE. The average molecular conformation of polyoxymethylene is modified from a uniform helix by intermolecular interaction⁸, but the degree of modification is much smaller than in PEO. The strong effect of intermolecular interaction in PEO crystals is considered to be responsible for \mathbf{u}_s of each atom in a molecule as well as the modification of the average molecular conformation.

Table 1 Integral intensities of Bragg reflections relative to the value at 25°C

Indices	-150°C	-100°C	-50°C	0°C	25°C	50°C
110	1.67	1.57	1.41	1.20	1	0.79
120	0.89	0.98	1.03	1.06		0.96
040, 200	0.78	0.89	1.05	1.05		0.94
$\bar{1}11$	1.34	1.44	1.44	1.27		0.85
021	1.06	1.18	1.29	1.16		0.94
111	0.89	1.11	1.14	1.11		0.94
121	1.34	1.44	1.43	1.26		0.91
112, 032, $\bar{1}32$						
$\bar{2}12, \bar{2}02$	0.94	1.11	1.14	1.12		0.95
052, $\bar{2}42, \bar{1}52$						
$\bar{3}12, 212$	0.59	0.83	0.96	1.04		0.91
152, $\bar{2}52$						
$\bar{3}32, 232$	0.62	0.93	1.08	0.98		1.05
023	0.86	1.04	1.20	1.13		0.94
033, $\bar{2}23$	0.76	1.01	1.18	1.07		0.93
113	1.22	1.46	1.40	1.21		0.78
$\bar{2}04, 004, \bar{1}24$	1.24	1.29	1.24	1.12		0.91
$\bar{2}14$	1.48	1.52	1.34	1.20		0.75
024, $\bar{2}24, \bar{1}34$	0.94	1.08	1.13	1.13		0.95
$\bar{2}34$	1.82	1.84	1.66	1.36		0.66
044, 124						
$\bar{2}44, \bar{3}24$	0.86	1.02	1.11	1.12		0.96
$\bar{2}35$	1.25	1.28	1.27	1.24		0.88
145, $\bar{1}65, \bar{4}25$	1.58	1.85	1.69	1.37		0.71
$\bar{3}55, \bar{2}65$	1.29	1.36	1.24	1.13		0.83
$\bar{2}36, \bar{3}16, \bar{1}36$	0.96	1.15	1.20	1.21		0.85
$\bar{2}56, \bar{1}56$						
$\bar{3}46, \bar{4}06$	1.62	1.72	1.55	1.32		0.80
136, 056	0.65	0.91	1.03	1.03		0.94
$\bar{3}56, \bar{4}36$	1.13	1.25	1.28	1.22		0.96
$\bar{2}07$	1.08	1.22	1.25	1.19		0.91
$\bar{1}17$	0.99	1.22	1.21	1.17		0.90
$\bar{1}27$	1.17	1.27	1.25	1.18		0.88
007, $\bar{1}37, \bar{3}27$	1.25	1.36	1.31	1.16		0.87
$\bar{2}47, \bar{3}37$	1.22	1.30	1.28	1.18		0.91
028, $\bar{1}48$						
408, $\bar{4}18$	1.21	1.38	1.39	1.24		0.86

In this paper a study of the reversible temperature change of u_s in PEO crystals is reported. X-ray diffraction experiments were made at several temperatures, and a model for the temperature change of u_s is proposed on the basis of the observed temperature changes of the integrated intensities of the Bragg peaks and the width of 120 reflection. Fourier analysis of the profile of 120 reflection was made to study the details of the correlation between u_s 's of different atoms.

EXPERIMENTAL

Samples were made from PEO films ($M_w \sim 6 \times 10^5$) drawn at room temperature about fivefold and then annealed at 55°C for one day.

X-ray scattering intensity was measured with a scintillation counter and a pulse height analyser for Ni filtered $\text{CuK}\alpha$ radiation. Integrated intensities of 31 Bragg peaks, which were strong enough for the counter method, were measured. A wide slit was used to let the whole beam of each Bragg peak pass through, and the average of the intensities of tails at both sides of the peak was subtracted as background scattering. Diffraction profiles of 120 reflection were measured at intervals of 0.1° in scattering angle.

The measurements were made over the temperature range from -150° to 50°C, a few degrees below the

premelting temperature. Temperature was controlled by blowing hot air or cold nitrogen gas over the sample. Temperature fluctuation was less than $\pm 1.5^\circ\text{C}$.

RESULTS

The observed integrated intensities at temperatures of -150°, -100°, -50°, 0°, 25° and 50°C are shown in *Table 1*, where the intensities at 25°C are set to unity. Temperature dependence of the integrated intensities is notable for two reasons. First, the magnitude of the intensity change does not increase monotonically with scattering angle. Some examples are given in *Figure 1*. Secondly, the integrated intensities of 25 Bragg peaks have their maxima at temperatures which differ from one peak to another.

Temperature dependence of the integral breadth of 120 reflection is shown in *Figure 2*. The integral breadth has a maximum around -75°C. Since the spacing of the planes (120) corresponds to the distance between the nearest-neighbour molecules as shown in *Figure 3*, the integral breadth gives information on the lateral molecular packing in the crystal.

The spacing of the planes (120) was estimated by fitting a quadratic curve to the diffraction profile around the maximum. It was found that the spacing changes smoothly with temperature, which suggests that there is no abrupt structural change within the temperature range concerned. All experimental results mentioned above are reproducible with temperature change.

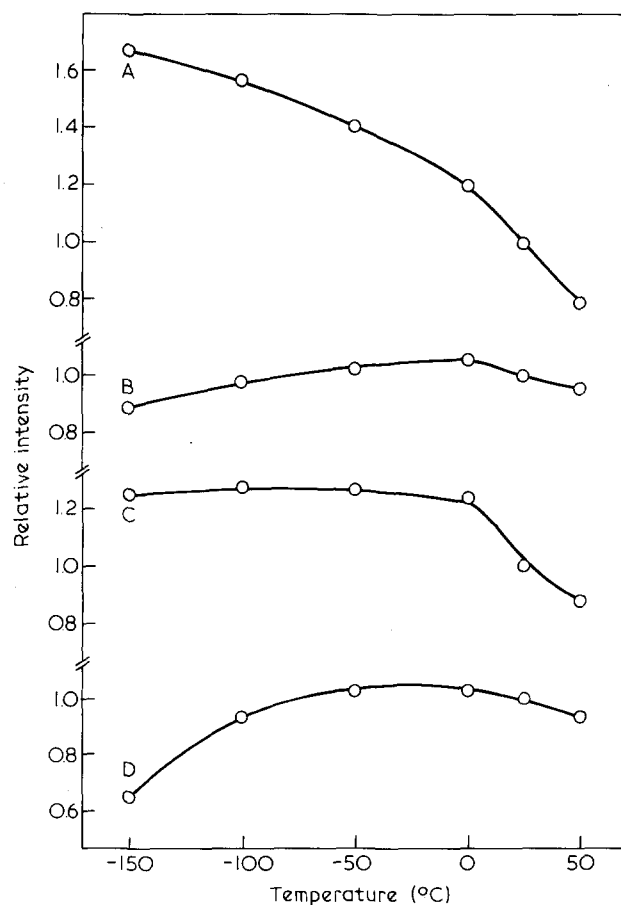


Figure 1 Relative integrated intensities: a, 110; b, 120; c, $\bar{2}35$; d, 136, 056

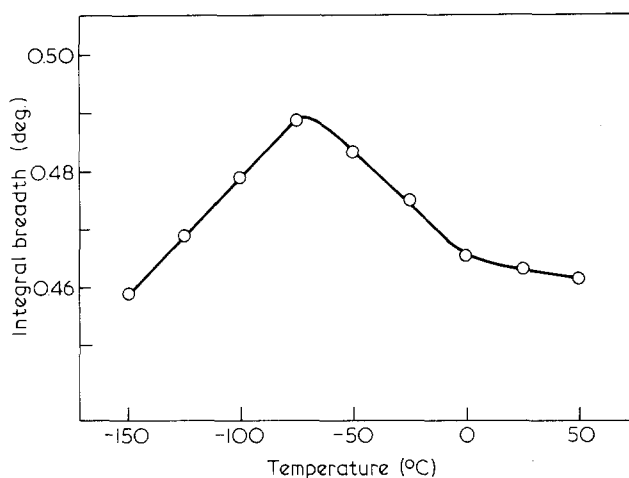


Figure 2 Integral breadth of 120 reflection. Values of integral breadth are given in terms of scattering angle and no correction is made for instrumental broadening

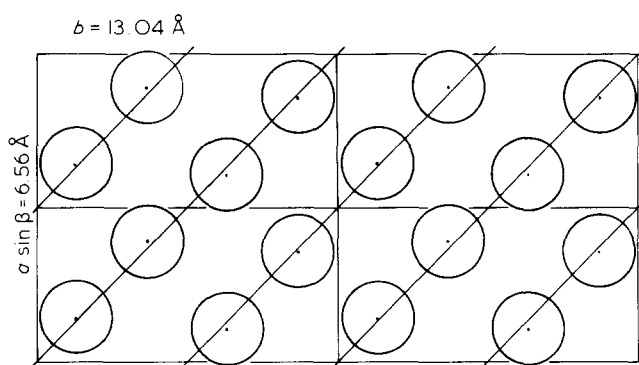


Figure 3 Four neighbouring unit cells, projected onto a plane perpendicular to the c -axis. Oblique lines and circles show the planes (120) and molecules, respectively

Temperature dependence of the coefficient B

The observed temperature dependence of the integrated intensities of the Bragg peaks suggests that the average molecular conformation changes with temperature. This will be seen by comparing the intensity change of 110 reflection with that of 120 reflection (Figure 1); they are quite different from one another. Such an aspect must be attributed to change of the crystal structure factor which reflects the average molecular conformation.

The value of B in equation (2) at each temperature can be obtained by referring to the result of structure analysis at room temperature¹. If average structure of a crystal is independent of temperature, integrated intensities at temperatures T_1 and T_2 of the j th Bragg peak ($I_j(T)$) will be connected by

$$I_j(T_2) = I_j(T_1) \exp\{-2[B(T_2) - B(T_1)](\sin \theta_j/\lambda)^2\} \quad (4)$$

where equation (2) is used. Temperature dependence of Bragg angle θ_j is neglected in equation (4). Summation of integrated intensities of all the Bragg peaks measured in electron units gives a definite value, which is determined by the chemical composition and $B(T)$, and is independent of the average atomic positions in a unit cell⁹. This is expressed formally by the equation

$$\sum_j I_j(T) = \sum_j I_j(T) \quad (5)$$

where the average molecular conformation for the left-hand side of equation (5) is different from that for the right-hand side, while the chemical composition and $B(T)$ are the same for both sides. Combination of equations (4) and (5) leads to

$$\sum_j I_j(T_2) = \sum_j I_j(T_1) \exp\{-2[B(T_2) - B(T_1)](\sin \theta_j/\lambda)^2\} \quad (6)$$

Through expansion of the exponential factor, equation (6) becomes

$$B(T_2) - B(T_1) = \frac{\sum_j I_j(T_1)[1 - I_j(T_2)/I_j(T_1)]}{2 \sum_j I_j(T_1)(\sin \theta_j/\lambda)^2} \quad (7)$$

The integrated intensities at room temperature and Bragg angles can be calculated from the crystal structure at room temperature¹. The ratios $I_j(T_2)/I_j(T_1)$ in equation (7) are shown in Table 1, which gives data on the strong Bragg peaks which are dominant in the summation in equation (7). Then one can calculate $B(T_2)$, setting T_1 to be room temperature.

The obtained $B(T)$ is shown in Figure 4. The curve has a minimum around -75°C . Rapid increase in the temperature range higher than 0°C is attributed to u_d , since 0°C corresponds to the temperature where narrowing of the n.m.r. absorption spectra begins¹⁰. On the other hand, large values in the low-temperature range cannot be explained by u_d and must be attributed to u_s .

Contribution of u_s to B (B_s) can be estimated on two assumptions; (1) the square of the amplitude of u_d is

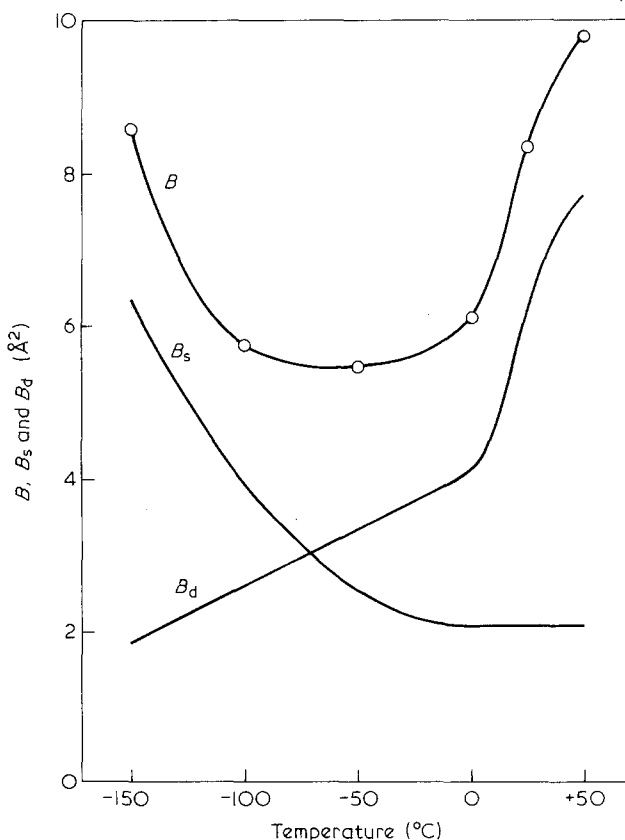


Figure 4 Temperature dependence of B , B_s and B_d

proportional to absolute temperature up to 0°C, and (2) u_s is constant above 0°C. The assumption (2) is supported by the fact that the integral breadth of 120 reflection, whose temperature dependence also reflects the change of u_s with temperature, is constant above 0°C. The curve of B against temperature T in Figure 4 up to 0°C is expressed very well by a quadratic function of temperature. From the assumption (1), B_d is linear with temperature, and B_s should be joined smoothly to the constant value (γ) above 0°C. Therefore B_d and B_s are expressed by the equations

$$\begin{aligned} B_d(T) &= \alpha(T + 273) \\ B_s(T) &= \beta T^2 + \gamma \end{aligned} \quad (T < 0^\circ\text{C}) \quad (8)$$

where α and β are constants, and temperature is measured in the centigrade temperature scale. The values of α , β and γ , which give the best fit through equation (3) are 1.5×10^{-2} , 1.9×10^{-4} and 2.1, respectively. Thus B is decomposed into B_s and B_d as shown in Figure 4. It is apparent that u_s plays an important role at low temperatures. In the following investigation will be confined to the temperature range below 0°C, in which thermal vibration is excited gradually with increasing temperature.

Fourier analysis

Since atomic position in a unit cell is determined by the molecular conformation and the molecular position, u_s is given by

$$u_s = u_{sc} + u_{sp} \quad (9)$$

where u_{sc} and u_{sp} are displacement of the atom due to distortion of the molecular conformation and displacement of the molecular position, respectively. Displacement of a molecule is considered to be strongly dependent on the surrounding molecular positions, and there will be some correlation among u_{sp} 's of different molecules, which is important for broadening of the Bragg peaks. It is assumed that u_{sp} is responsible for both the depression of the integrated intensities and the broadening of the Bragg peaks, while u_{sc} is responsible for only the intensity depression. Then the broadening of 120 reflection gives information about deviation of the intermolecular distance from the average value: the spacing of the planes (120) (Figure 3).

Fourier analysis of the profile of 120 reflection was made by the method of Warren and Averbach¹¹. However, it is more simplified and only the ratio of the Fourier coefficients at different temperatures is treated. Although the simplification gives quantitatively poorer results, it greatly reduces the experimental and analytical difficulties; further, some valuable information can be deduced even when higher orders of a strong reflection are not observed as in this case.

The cosine Fourier coefficient A_n of an observed profile is given by

$$A_n = A_n^c A_n^i \quad (10)$$

where A_n^c and A_n^i are the cosine Fourier coefficients of the crystalline diffraction and instrumental broadening, respectively, which are assumed to be symmetric. Since temperature dependence of A_n^i is negligible, the ratio

between A_n 's at temperatures T_1 and T_2 is given by

$$\frac{A_n(T_2)}{A_n(T_1)} = \frac{A_n^c(T_2)}{A_n^c(T_1)} \quad (11)$$

Following Crist and Cohen⁶, A_n^c is given by

$$A_n^c = \exp(-n/\bar{N}) \exp(-2\pi^2 m^2 \langle Z_n^2 \rangle) \quad (12)$$

where \bar{N} is the number average crystal size in terms of the number of molecules, and m the order of the reflection. If u_{sp} contributes only to broadening of the Bragg peaks, the mean square deviation of the intermolecular distance between the n th neighbours will be given by $\langle Z_n^2 \rangle d^2$; d is the average distance between the nearest-neighbour molecules. However, if u_{sp} is responsible for the intensity depression as in this case, contribution to B_s is reduced from u_{sp} in calculation of $\langle Z_n^2 \rangle$. In equation (12) it is assumed that the distribution of the deviation of the intermolecular distance is Gaussian for every n . Substituting equation (12) into (11) and taking logarithms one obtains

$$\begin{aligned} -\frac{1}{2\pi^2 m^2 n} \log \left(\frac{A_n(T_2)}{A_n(T_1)} \right) \\ = \frac{1}{n} (\langle Z_n(T_2)^2 \rangle - \langle Z_n(T_1)^2 \rangle) + \frac{1}{2\pi^2 m^2} \left(\frac{1}{\bar{N}(T_2)} - \frac{1}{\bar{N}(T_1)} \right) \end{aligned} \quad (13)$$

Fourier coefficients are calculated through linear interpolation of the data obtained by a step-scan method and correction for background scattering by a baseline method. Although such a calculation includes some errors in quantitative discussions, one can get qualitative characteristics of u_{sp} . No correction is made for the changes of the structure factor and Lorentz, polarization and absorption factors within the diffraction peak, since their influences on the A_n 's are negligible. The hook effect, the error due to underestimation of the tails of the diffraction peaks⁶, is cancelled sufficiently by dealing with the ratio of the A_n 's.

The values of the left-hand side of equation (13) are plotted against n in Figure 5. The standard temperature T_1

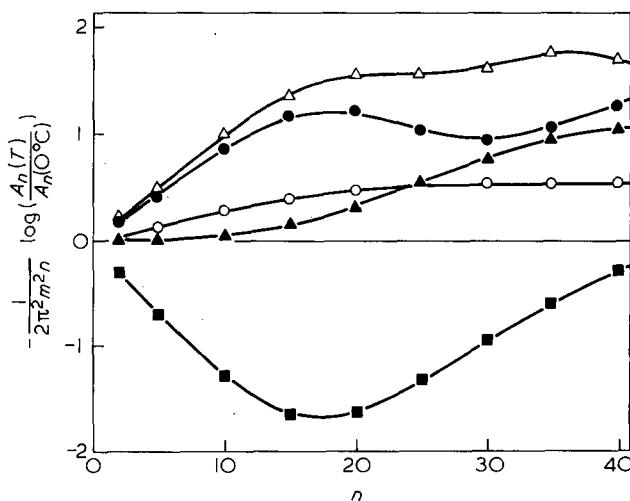


Figure 5 Dependence of $(-1/2\pi^2 m^2 n) \log [A_n(T)/A_n(0^\circ\text{C})] \times 10^{-4}$ on n : ■, -150°C; ▲, -125°C; ●, -100°C; ▽, -75°C; ○, -50°C

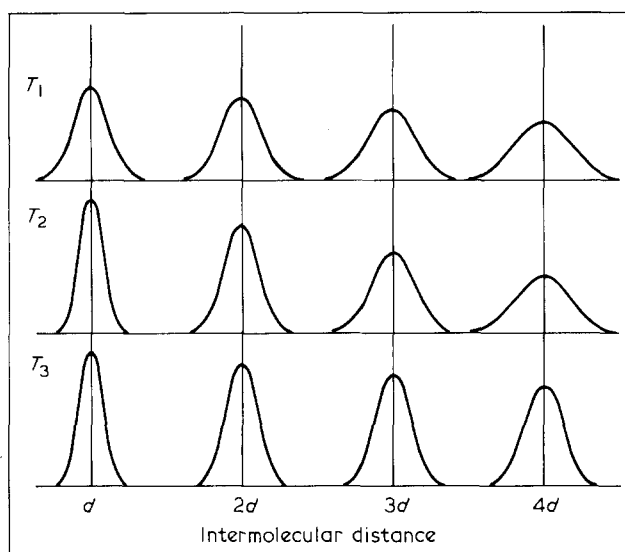


Figure 6 Schematic pair correlation functions of molecular positions at temperatures T_1 , T_2 and T_3 ($T_1 < T_2 < T_3$). The ordinate represents the fraction of the molecular pairs separated by the distance represented by the abscissa

is 0°C and m is unity in this case. Since \bar{N} is independent of n , the n dependence of the curves is attributed to the first term on the right-hand side of equation (13). The fact that the extrapolated curves to $n=0$ pass near to the origin implies that the second term in equation (13) is negligible; change of the crystal size is very small.

A model for the temperature dependence of u_s

The conformation and position of molecules in a crystal are assumed to be essentially determined so that total energy E of the crystal, which is given by the sum of intramolecular (E_1) and intermolecular (E_2) interaction energies, may be a minimum. The total energy is written as

$$E = \sum_i E_1(x_i) + \sum_{i \neq j} E_2(x_i, x_j, r_{ij}) \quad (14)$$

where x_i is the set of internal coordinates of the i th molecule and r_{ij} is the set of variables describing the relative position of the i th and j th molecules. If E_2 is independent of x_i and x_j , equation (14) will give a perfect crystal; molecules with the conformation determined by E_1 are arranged on the lattice points determined by E_2 . However, in a real crystal E_2 depends on x_i and x_j , and the most stable structure may be a distorted one. This is the case in PEO crystals, in which the conformation dependence of E_2 is important⁷.

The change of the average crystal structure with temperature suggests that E_2 depends on temperature; further, temperature changes of B_s and the integral breadth of 120 reflection are considered to be introduced by the temperature dependence of E_2 . The conformation dependence of the interaction energies is obscured by a smearing-out effect due to thermal vibration. The smearing-out effect is more remarkable on E_2 than on E_1 , since change of relative position between a pair of atoms due to thermal vibration is larger for atoms belonging to different molecules than for atoms in the same molecule. It is consistent with the results of infra-red absorption measurement by Yoshirhara *et al.*¹²; they reported that a few absorption bands split at a low temperature

($\sim -130^\circ\text{C}$) and attributed it to temperature dependence of the intermolecular interaction. Thus, with increasing temperature, the conformation dependence of E_2 becomes weaker and u_s , both u_{sc} and u_{sp} in equation (9), decreases.

Decrease of u_s with increasing temperature will readily mean decrease of B_s . The integral breadth of 120 reflection, which has a maximum as shown in Figure 2, can also be explained by the monotonic decrease of u_s . Since the molecules are arranged almost on the planes (120) (Figure 3), u_{sp} , which is responsible for the broadening of the diffraction profile, can be expressed in terms of the pair correlation function of the molecular positions on the planes as shown in Figure 6. The broad peaks show that the crystals are distorted, and their width increases with the distance between the origin and the centre of the peak, which corresponds to a decrease in crystalline order at long range. This increase of the peak width in the pair correlation function broadens the profile of 120 reflection. It should be noted that, as the peak widths increase with the distance more rapidly, the diffraction profile becomes broader. It is reasonable to assume that at short range, deviation of intermolecular distance due to u_{sp} decreases at lower temperature than at long range, as illustrated in Figure 6, in which, as temperature is raised from T_1 to T_2 , each peak at short range becomes narrower whereas those at long range remain unchanged. In other words the peak widths increase more rapidly at T_2 than at T_1 . As temperature is raised further towards T_3 , narrowing of the peaks at long range takes place, and the increasing ratio of the peak widths come to increase slowly again. Then the width of the diffraction profile, has a maximum at T_2 ; this corresponds to the observed temperature dependence of the integral breadth of 120 reflection.

Details of u_{sp}

The increase of the peak width in the pair correlation function is reflected in the n dependence of $\langle Z_n^2 \rangle$ in equation (13). The result of Fourier analysis (Figure 5) suggests that, for small n up to ~ 20 , $\langle Z_n^2 \rangle$ is proportional to n^2 at all temperatures. For large n above ~ 20 , the n dependence of $\langle Z_n^2 \rangle$ changes from n^2 to n with increasing temperature towards -75°C and proportionality to n is dominant above -75°C .

For two important cases, the n dependence of $\langle Z_n^2 \rangle$ is known¹³. When, in each crystal, the molecules are arranged on lattice points of a reference lattice, which is perfect but whose lattice constants are different from one crystal to another, $\langle Z_n^2 \rangle$ is proportional to n^2 . For the other case that the reference lattice is a paracrystal type, which is common for all crystals, $\langle Z_n^2 \rangle$ is proportional to n . Then the n dependence of $\langle Z_n^2 \rangle$ is considered to change from n^2 to n , as the crystalline order is progressively lost. Even if the crystals suffer from further distortion, thermal vibration and the static displacement of the frozen thermal vibration type around the lattice points of the reference lattice, the n dependence of $\langle Z_n^2 \rangle$ is not changed.

The observed n dependence of $\langle Z_n^2 \rangle$ suggests that the perfect reference lattice is applicable in a region of about 20 molecules or more in diameter, which is smaller than the crystal size estimated at more than 50 molecules in diameter from the data on other materials^{3,6,14}. One can consider that a crystal, which is coherent for X-ray scattering as a whole, is composed of several domains with respective perfect reference lattices (local reference

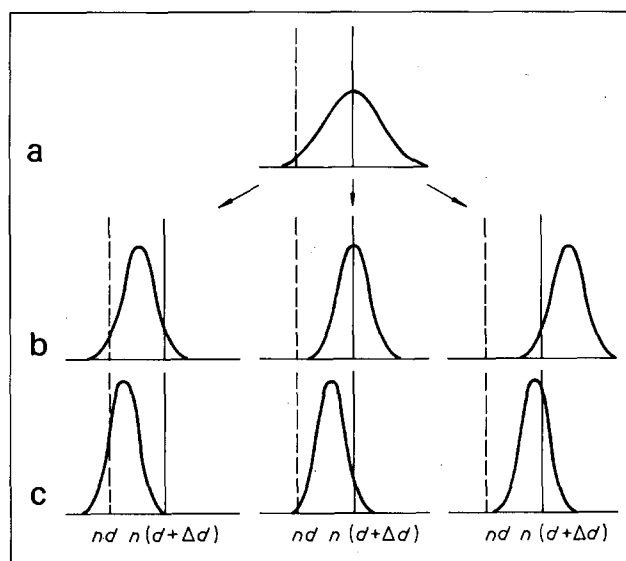


Figure 7 Schematic temperature changes of the n th peak of the pair correlation function for domains with lattice constant $(d + \Delta d)$ at temperature T_1 (a) T_1 , (b) T_2 , (c) T_3

lattices), whose lattice constants are different from each other. The crystalline order is maintained within each domain and is lost at long range. The temperature change of $\langle Z_n^2 \rangle$ up to $n \approx 20$ is attributed to a change in the distribution of the lattice constants of the local reference lattices, which becomes wider below -75°C and narrower above -75°C with increasing temperature. Above $n \approx 20$, the temperature change of $\langle Z_n^2 \rangle$ is caused by a change of the domain size, which decreases monotonically up to -75°C and is constant above -75°C , ~ 20 molecules in diameter.

With the aid of the local reference lattice, decrease of u_{sp} , static displacement from the average crystal lattice over all crystals in the sample, caused by the smearing-out effect is known to occur in two stages. First, the static displacement from the lattice points of the local reference lattice decreases, and next the distribution of the lattice constants of the local reference lattices becomes narrower. A schematic illustration of this model is given in Figure 7 in terms of the pair correlation function of the molecular position on the planes (120). The peak in Figure 7a shows the distribution of the distances between the n th neighbour molecules in certain domains whose lattice constants are deviated by Δd from the average value d over all crystals in the sample (nd is smaller than the size of the domains). As temperature is raised towards T_2 , the number of molecules which compose one domain becomes smaller and the lattice constants of some of the domains become a little larger or smaller than $(d + \Delta d)$ in order to make the static displacement from the lattice points of the local reference lattices decrease. Through this splitting of the lattice constants, overall distribution of the lattice constants becomes wider, but the peak width of the pair correlation function decreases because of a large decrease of the static displacement from the local reference lattices. At this stage the smearing-out effect is limited to a small region.

At temperature T_3 , the smearing-out effect is so strong that the structural characteristic of each domain may be obscured. The lattice constants of all local reference lattices approach the average value d , and the distribution of the lattice constants becomes narrower. The smearing-out effect is saturated above 0°C .

DISCUSSION

Three-dimensional periodicity of the molecular arrangement in crystals is required to avoid intermolecular interactions with high energies. However, construction of a completely periodic structure is difficult in polymer crystals for two reasons. First, the molecular conformation, which gives the best packing in a crystal, is often different from the stable conformation of an isolated molecule; the latter does not need to have translational periodicity along the molecular axis. Secondly, the degree of freedom of a molecule is restricted by the chemical bonds; a structure which gives favourable molecular packing in a certain small part may prevent good packing in other parts. Then polymer crystals often suffer from some distortion due to intermolecular interaction, even if they are large and dislocation-free. In this sense it can be called intrinsic (static) distortion.

It has been reported through Fourier analysis that the dislocation model for u_s ¹⁵ (extrinsic distortion) may be applied to PE⁶ and PTFE.¹⁶ The extrinsic distortion due to dislocations possibly exists in PEO crystals, too, but its effect on the temperature change of X-ray diffraction is negligible compared with the intrinsic one. The study of the distortion in polystyrene crystals through Fourier analysis¹⁴ seems to show that both the intrinsic and the extrinsic distortions are important for polystyrene crystals.

ACKNOWLEDGEMENTS

The author would like to thank Prof. K. Asai and Dr H. Miyaji for their continued encouragement and helpful suggestions.

REFERENCES

- 1 Takahashi, Y. and Tadokoro, H. *Macromolecules* 1973, **6**, 672
- 2 Ruland, W. *Polymer* 1964, **5**, 89
- 3 Katayama, K. *J. Phys. Soc. Jpn.* 1961, **16**, 462
- 4 Yamamoto, T. and Hara, T. *Polymer* (in press)
- 5 Kulshreshtha, A. K. and Dwelts, N. W. *Acta Crystallogr. A* 1971, **27**, 670
- 6 Crist, B. and Cohen, J. B. *J. Polym. Sci., Polym. Phys. Edn.* 1979, **17**, 1001
- 7 Kusanagi, H., Tadokoro, H. and Chatani, Y. *Rep. Prog. Polym. Phys. Jpn.* 1975, **18**, 193
- 8 Saruyama, Y., Miyaji, H. and Asai, K. *J. Polym. Sci., Polym. Phys. Edn.* 1979, **17**, 1163
- 9 Ruland, W. *Acta Crystallogr.* 1961, **14**, 1180
- 10 Hikichi, K. and Fruichi, J. *J. Polym. Sci. A* 1965, **3**, 3003
- 11 Warren, B. E. and Averbach, B. L. *J. Appl. Phys.* 1950, **21**, 595
- 12 Yoshihara, T., Tadokoro, H. and Murahashi, S. *J. Chem. Phys.* 1964, **41**, 2902
- 13 Takahashi, H. *J. Phys. Soc. Jpn.* 1969, **27**, 708
- 14 Buchanan, D. R. and Miller, R. L. *J. Appl. Phys.* 1966, **37**, 4003
- 15 Rothma, R. L. and Cohen, J. B. *J. Appl. Phys.* 1971, **42**, 971
- 16 Wecker, S. M., Cohen, J. B. and Davidson, T. *J. Appl. Phys.* 1974, **45**, 4453